Effect of Monoethanolamine Content on the Crystallinity of ZnO Thin Films

Ahmet TUMBUL[*1]

1Harran University, Research Centre for Sci. and Technol., 63300, Sanliurfa, Turkey

corresponding author e-mail: atumbul@harran.edu.tr

Abstract: ZnO is one of the most widely used semiconductors for opto-electronic applications due to its tunable band gap energy, high optical transparency in visible region. The effect of different monoethanolamine (MEA) ratio on structural, morphological and optical properties of ZnO thin films was investigated in this study. A nano-fiber like structured ZnO was fabricated through facile sol-gel dip coating process on glass substrates without any further treatment. We observed that the peak intensity of samples increased and the amount of defects in the crystal could be further decreased by rising its of monoethanolamine. Besides, the micro-fiber like grains of the ZnO covered the glass surface quite densely when the monoethanolamine content increased. The optical study showed that the transparency of the films could be enhanced by increasing the amount of stabilizer.

Keywords: ZnO, Thin films, Sol-gel method, Photoluminescence, Opto-electronic

Monoetanolamin Miktarının ZnO İnce Filmlerin Kristallenmesi Üzerine Etkisi

Özet: Çinko oksit yarıiletkeni sahip olduğu değiştirilebilir yasak enerji aralığı ve görünür ışık bölgesindeki yüksek optik geçirgenliğinden dolayı opto-elektronik uygulamalar için çok sık kullanılan yarıiletkenlerden biridir. Farklı miktarlarda kullanılan monoethanolamin miktarının ZnO ince filmlerin yapısal, morfolojik ve optik özellikleri üzerine etkileri bu çalışmada incelenmiştir. Nano-fiber yapılı ZnO ince filmler başka herhangi bir işlem gerektirmeden cam altlık üzerine, basit sol-jel daldırma yöntemi kullanılarak sentezlenmiştir. Monoetanolamin miktarı artırıldığında örneklerin XRD pik şiddetlerinin arttığı ve kristal kusurlarının azaldığı gözlemlenmiştir. Bunun yanında, monoetanolamin miktarı arttığında mikro-fiber ZnO taneciklerinin altlık yüzeyini oldukça yoğun bir şekilde kapladığı görünmüştür. Ayrıca optik ölçümler sonucu stabilizer olarak kullanılan monoetanolamin miktarının artışı ile ince filmlerin görünür ışık bölgesindeki geçirgenliğinin arttığı görülmüştür.

Anahtar kelimeler: ZnO, İnce filmler, Sol-jel metodu, Fotoluminesans, Opto-elektronik

Ahmet TUMBUL, atumbul@harran.edu.tr, ORCID: https://orcid.org/ 0000-0003-3790-9667

1. Introduction

Among the many metal-oxide materials, ZnO has attracted attention due to its unique physical properties such as the wide band gap value, high optical transparency along the visible range, good piezo-electric behavior by means of orientation throughout c-axis, high electron mobility and an exciton binding energy value of 60 meV. In view of its tunable electrical, optical and morphological properties, ZnO has been used as a semiconductor material in many application areas including electronics, opto-electronic displays technologies, gas sensing materials [1-5]. In addition, un-doped and doped n-type ZnO have been used as photo-diodes and in solar cells applications as window layer, buffer layer and alternative transparent conductive oxide (TCO) layer. Specifically, the TCO obtained by metal doping, are used instead of ITO which is rarely found in nature [6-8].

There is a number of studies about fabrications and application of ZnO thin film material. Both vacuum based and solution-processed thin film deposition methods have been used by researchers, extensively. Magnetron sputtering [9], pulsed laser [10] and plasma-assisted molecular beam epitaxy [11] are the most widely-known vacuum based deposition techniques to manufacture ZnO thin films. On the other hand, simple and multi-functional chemical deposition methods have also been widely used recently. Silar [12], spray pyrolysis [13], chemical bath deposition [14] and sol-gel methods [15] are among the most prominent non-vacuum process thin film deposition techniques. Of these deposition techniques, sol-gel has been in consideration widely due to its versatile and utilizable properties such as allowing to control of solvent and precursors, molar composition regulation, manipulation of surface morphology, being suitable for large area coatings for mass-production through low-cost equipment [16, 17].

To get appropriate material properties, many studies were conducted related to ZnO semiconductors. For instance, Saeed et al [18] prepared ZnO films by dip and spin coating methods. According to this study, the dip-coated ZnO with 6.5 pH value has the largest transmittance in visible range as high as 92%. Makino et al [19] obtained the magnetron sputtered ZnO and DC-magnetron sputtered Ga doped ZnO thin films. In this study, significant differences in electrical properties of ZnO were observed depending on the deposition conditions and gallium dopant effect. The structural properties of ZnO films can be manipulated easily by using chemical deposition methods. Aslan et al. [20] were synthesized ZnO thin films by the sol-gel dip-coating process, using two different zinc salts, namely zinc-nitrate tetrahydrate and zinc-chloride. When the former precursor was used, a dense granular surface structure was obtained. However the zinc-oxide nanorod arrays were obtained when the latter was used as the precursor. Soylu et al. [21] produced ZnO nanofiber at various molar ratios and observed major differences in structural and electrical properties of ZnO thin films and its diode application by sol-gel spin coating method. Not only the different precursors and molar ratios, but also the complex-agent and additives play a major role in obtaining effective and high performance materials. For example, Golobostanfard et al [22] obtained dip-coated ZnO thin films using different types of additives. In this report, physical and chemical properties of zinc-oxide materials were investigated and were found to depend on different additives. Indeed, amino groups have strong effect on the physical properties and stability of the zinc-oxide materials. Vila et al [23] investigated solution stability of sol-gel ZnO Ink by using ethanolamine agent. Besides, a weak base triethanolamine (TEA) with varying concentrations was used to enhance physical properties of ZnO thin films as reported by Metha et al [24]. Our motivation in this study is to examine the effect of the amount of monoethanolamine (MEA) which is a stabilizer base, on the surface morphology as well as, the optical and structural properties of facile and green sol-gel deposited ZnO thin films.

2. Material and Method

The flow-chart of the synthesis and deposition conditions of ZnO thin films are given in Figure 1. 1.646 g of zinc nitrate tetrahydrate (0.0075 mol) ($Zn(NO_3)_2.4H_2O$) was dissolved in 38 ml ethylene glycol monomethly ether [$CH_3OCH_2CH_2OH$]. Then, different amounts of monoethanolamine were added into the solution. All purchased chemicals and solvent were used without any further purification. The ZnO1, ZnO2, ZnO3 and ZnO4 corresponded to the thin films which were obtained by adding 0.25, 0.5, 0.75 and 1 ml monoethanolamine, respectively. All solutions were stirred at room temperature overnight. A computer-controlled dip-coater system was used to obtain thin films. Further details of the synthesis of the solutions and thin film preparation can be found in a previous study [20]. In order to observed ethanolamine effect, the films were 20 times coating layer for all the samples.

The crystallinity and crystalline parameters of ZnO thin films were determined using Rigaku Ultima III X-ray Diffractometer with monochromatic Cu Kα Radiation, λ=0.154 nm. The Raman spectroscopy (Renishaw/inVia spectrometer with a Nd:YAG laser, 532 nm, 100mW) was used to best understand the ZnO structure. The X-ray photoelectron spectroscopy (XPS) measurement was carried out to get the chemical binding energy of ZnO thin film. Scanning Electron Microscope (Zeiss Evo 50 model SEM) was employed to investigate the material's surfaces morphology. In order to understand the optical properties of ZnO thin films, transmittance and absorbance spectra of the samples were studied by using a double beam UV-Vis Spectrometer (Perkin Elmer 45 UV-Vis). In addition to this, the PL spectrum of ZnO thin films were carried out by UV-VIS-NIR spectrophotometer (Shimadzu, UV-3600 plus).
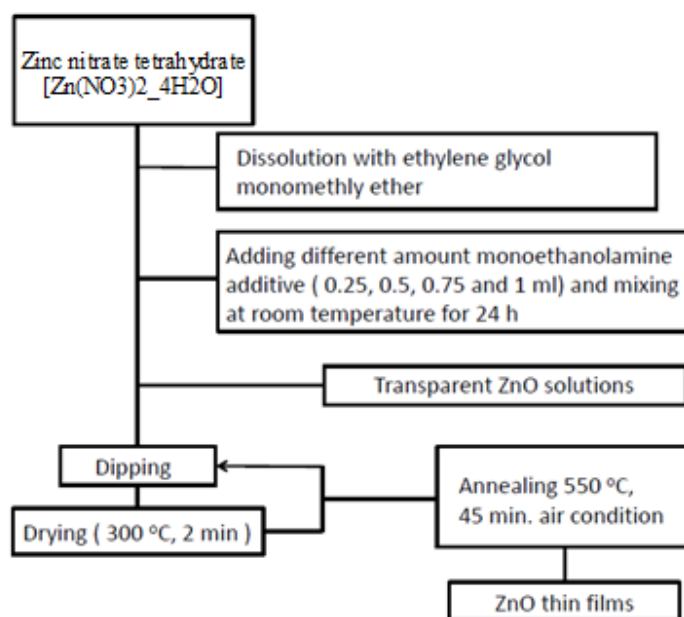

Figure 1. Flow-chart of synthesis of ZnO solutions and thin film processes

3. Results

3.1. Structural properties

The XRD spectrum of ZnO thin films which were grown on the soda-lime glass substrates and annealed at 550 °C, in air atmosphere were given in Figure 2. Number of X-ray photons which incident on the unit area of sample has been fixed during the measurements for all the samples. The strong XRD peak of ZnO thin films which located (002) miller plane, indicated the samples showed polycrystalline nature with

hexagonal crystal structure with strongly preferred orientation throughout the c-axis (JCPDS card no: 00-036-1451). We observed that the peak intensity of the ZnO thin films which were obtained by using zinc-nitrate salt were stronger in comparison to other studies done by sol-gel methods [25, 26]. In addition, the peak intensity and sharpness of the FWHM of the ZnO thin films increased when the additive content increased. The use of stabilizer and salt source are two factors playing major role in the growth mechanism. According to Golobostanfard et al, zinc-nitrate based salts can be easily converted to zinc hydroxy double salt in sol and this convertion increased the solution pH value. Hence, a high quality crystal structure can be obtained by controlling pH level and additive content [22, 27].

Equation 1 was used to determine c constant of the ZnO thin films. The d_{hkl} inter-planar distance was determined for (002), Miller indices by using Bragg's Law [28]

$$\frac{1}{d_{(hkl)}^2} = \frac{4}{3}\left(\frac{h^2 + hk + k^2}{a^2}\right) + \frac{l^2}{c^2} \tag{1}$$

The values of c lattice parameters were found to be roughly ~5.224 Å, ~5.231 Å, ~5.207 Å and ~5.207 Å, which correspond to the thin films ZnO1, ZnO2, ZnO3 and ZnO4, respectively.

To calculate the crystallite size of the ZnO films, the Scherer's formula was used [29],

$$D_{hkl} = \frac{K\lambda}{\sqrt{\beta_o^2 - \beta_i^2}\cos\theta} \tag{2}$$

where λ is the X-ray wavelength, θ is Bragg's angle of the corresponding diffraction peak, K is the Scherer constant, β_o is the FWHM of characteristic (002) peak of ZnO materials and β_i is the instrumental broadening of the used diffractometer. We observed that the ZnO crystallite size increased as the monoethanolamine content increased. The observed results were consistent with X-ray spectra of the samples.
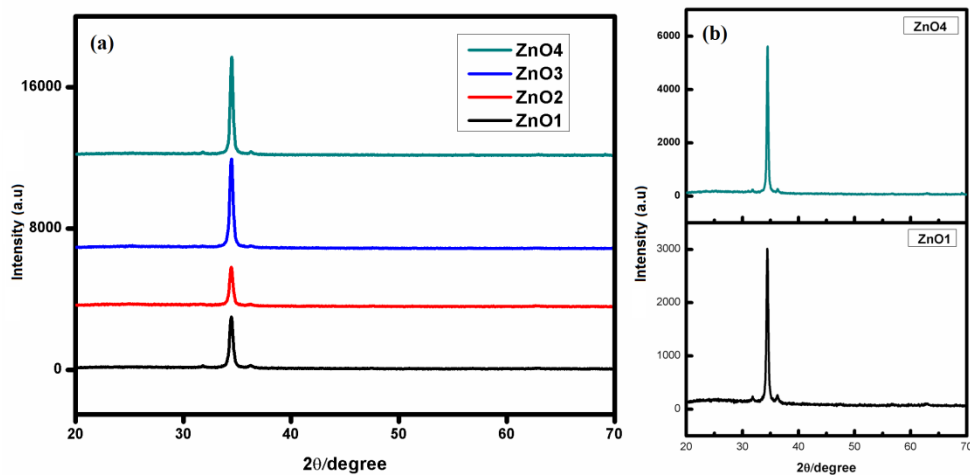

Figure 2. (a) XRD specta of ZnO thin films **(b)** Peak intensity difference between ZnO1 and ZnO4 depends on monoethonolamine content

The dislocation density (δ) which is a result of the defects centers in the crystal was calculated using Equation 3 [28],

$$\delta = \frac{1}{D^2} \tag{3}$$

where D is the crystallite size of ZnO. The highest dislocation density value was found to be about $\sim 4.2 \times 10^{-4}$ nm^{-2} (see Table 1). Bindu and Thomas calculated dislocation density of ZnO nanoparticles. According to this calculation, our synthesis ZnO thin film samples have the lowest value in the literature. As such, we concluded that the crystal quality increased when the defect amount in crystal decreased [28]. Further details of the structure parameters can be found in Table 1.

Table 1. The crystal parameters of ZnO samples

Sample series	(002) peak position (2θ)	Interplanar spacing d_{100} (Å)	Lattice constant c (Å)	D (nm)	Dislocation density (δ) (nm^{-2})	FWHM
ZnO1	34.441	2.6019	5.224	23.8	0.0420	0.368
ZnO2	34.440	2.6020	5.231	23.9	0.0418	0.367
ZnO3	34.460	2.6005	5.207	24.7	0.0404	0.356
ZnO4	34.480	2.6005	5.207	29.5	0.0338	0.306

In addition to XRD analysis, the Raman measurements have also been carried out in order to best understand the molecular vibrations and other impurity phase identification in the ZnO thin films. The micro-Raman spectrum of ZnO1 is presented in Figure 3. The main peaks were found for ZnO thin film which was located at 430 cm^{-1}, 568 cm^{-1} and 1100 cm^{-1} identified a wurtzite structure ZnO. The Raman results are consistent with the literature [30, 31]. According to Zhang et al [32], the broad peaks that located at 568 cm^{-1} and 1100 cm^{-1} attributed to the 1LO(E_1) and 2LO vibration modes of wurtzite ZnO.
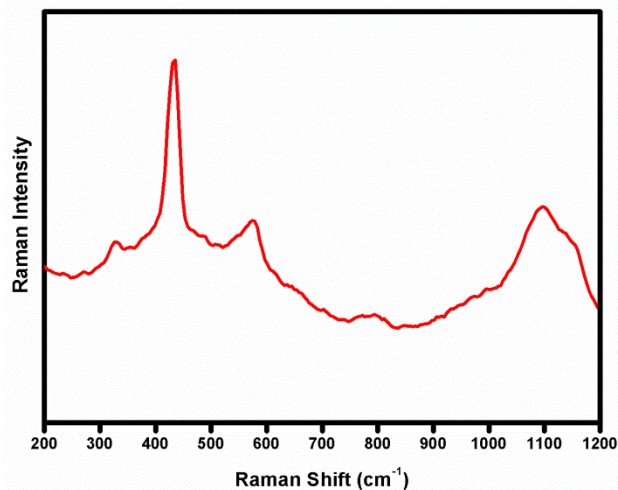

Figure 3. Raman spectrum of ZnO1 thin film

In order to best understand the chemical composition of ZnO thin film, the X-ray photoelectron spectroscopy (XPS) was used. Figure 4. shows the binding energy values of Zn 2p and O 1s core levels of ZnO1 thin film. As seen in Figure 4. the obtained binding energies at $\sim$1021 eV and $\sim$1044 eV corresponding to the Zn 2p$_{3/2}$ and Zn 2p$_{1/2}$ peaks, respectively. The presence of oxygen is confirmed by main peak which located at the $\sim$529 eV. It ascribed to the O^{2-} (O1) ion in the host ZnO structure [2,17].
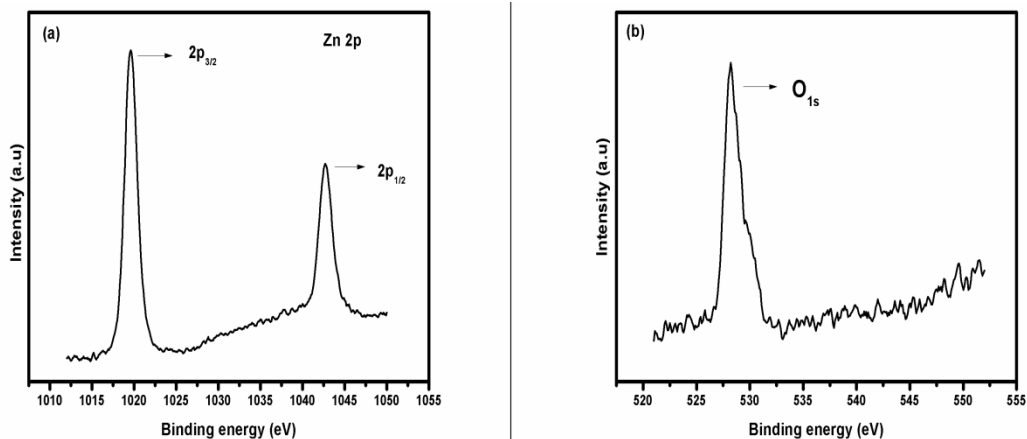
Figure 4. Wide-scan XPS spectra of the ZnO1 thin film

3.2. Morphological studies

Figure 5 shows the surface morphology of ZnO semiconductors obtained by using various monoethanolamine content. It can be seen from the SEM micro-graphs of thin films that, the films covered the surface homogeneously and smooth surfaces was observed without any cracks. The micro-fiber like structured ZnO grains become denser when the monoethanolamine content was increased. The presence of amine groups increases with pH of the solutions [33]. Thambidurai et al. [34] observed a similar effect on sol-gel deposited ZnO thin films. According to this study, when the pH of ZnO solutions increased from 4 to 10, the crystal quality and grain size of ZnO enhanced. The X-ray studies confirmed this phenomenon. The micron-size grains made up of the nano-size particles according to the Ostwald principle. The nano-size particles combined rapidly and the most stable micro-sized structured occurred [33].
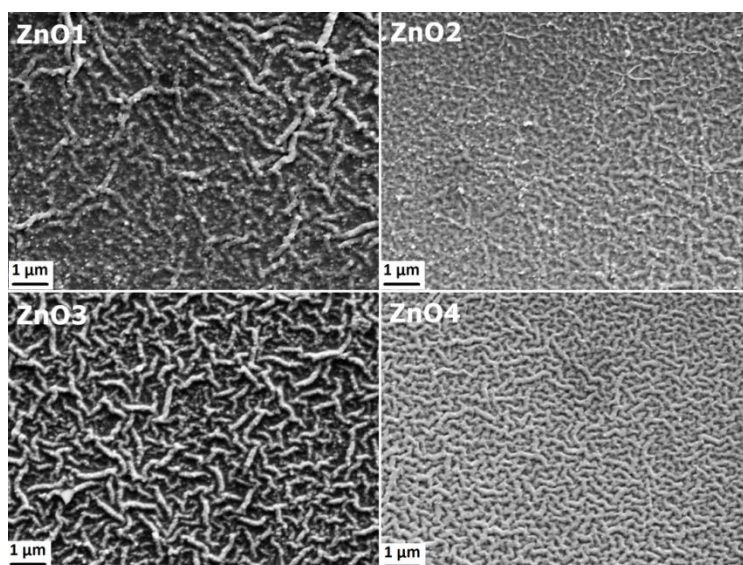

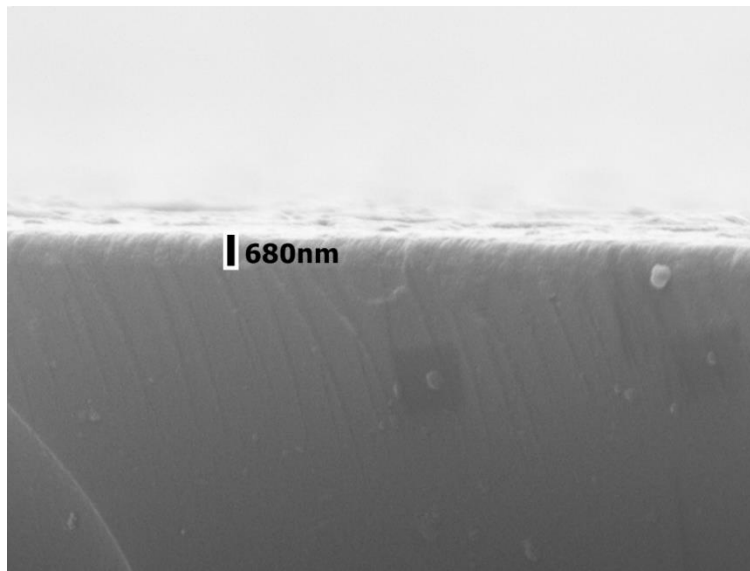**Figure 5.** Surface images of ZnO samples

Figure 6. Cross-section images of ZnO1 thin film

The film thickness of ZnO sample was determined by means of SEM tool. Figure 6 shows the cross-section of ZnO1 thin film. From the cross-section of the SEM images, the thickness of ZnO sample is approximately 680 nm.

3.3. Optical studies

The transmittance spectra of ZnO samples were performed in the wavelength range of 300 and 1200 nm (Figure 7). The optical transparency of ZnO samples increased when the amino content was increased. Indeed, the alkanolamines groups with zinc acetate salt provide a clear solution [33]. This significant rising in visible region is very important for using ZnO materials as transparent conductive oxide materials for solar cell applications. The band gap energy of ZnO films was derived from absorbance spectrum by using the Tauc formula [35].

$$\alpha h\nu = A\big(h\nu - E_g\big)^x \tag{4}$$

where A is a random constant, h is the Planck constant, α is the absorption coefficient, $x = 1/2$ for allowed direct band transition, and E_g is the band gap energy value. Figure 7 shows band gap energy values of ZnO samples which were calculated roughly as 3.11, 3.15, 3.19 and 3.18 eV for ZnO1, ZnO2, ZnO3 and ZnO4 samples, respectively. It was clearly seen that the band gap energy of ZnO thin films, except of ZnO4, shifted a small amount towards higher energy values with increasing the amino contents. However, the band gap of ZnO4 sample was found to be lower than ZnO3 samples. As mentioned above, the crystallinity of the ZnO samples improved when the amino content increased. So, the decrease of band gap of ZnO4 sample was compared with the ZnO3 sample which was attributed to larger grain size in the crystal [31,34]. The calculated crystallite size of samples which given the Table 1, have strengthen of band gap shifts.
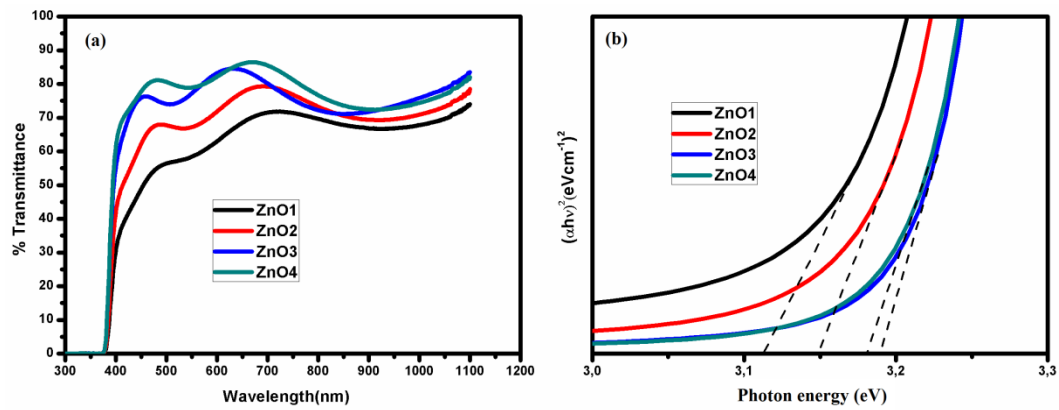
Figure 7. Transmittance spectrum **(a)** and band gap energy **(b)** of ZnO samples

Figure 8 shows the photoluminescence (PL) spectra of ZnO samples which were prepared in different monoethanolamine contents, carried out at room temperature. The UV emission around 380 nm was observed in all of the samples and was attributed to the free excitonic emission and bound excitonic emission due to some defects in the crystal [13]. Reduction of PL peak intensity was attributed to the decreasing of non-radiative recombination in visible range. Our observation is in a good agreement with previous work [21]. Indeed, the dislocation density calculation showed that the defect level in the crystal was related to the ultraviolet emission. We conclude that when the monoethanolamine content increased, the defect centers in the crystal and the proportionally nonradiative recombination were decreased.
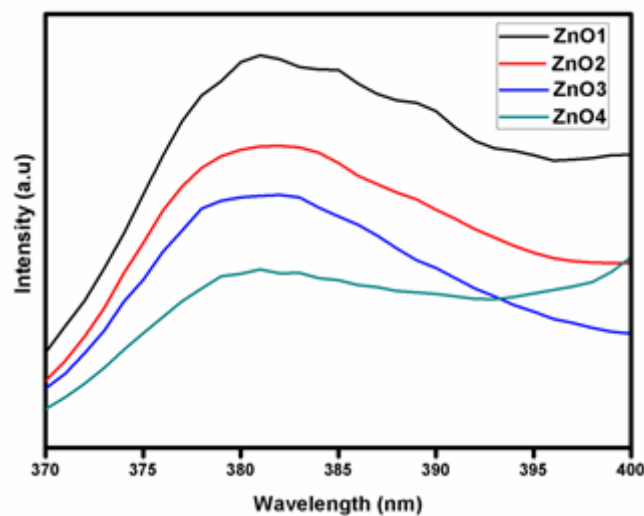

Figure 8. PL spectrum of ZnO thin films

4. Conclusion and Comment

The XRD main peak rising was observed when the monoethanolamine content increased from 0.25 to 1 ml. The SEM micrographs showed that the surface density of the samples increased with rising of stabilizer content. The most desired transparency was obtained by ZnO4 samples which was obtained by using 1 ml monoethanolamine. Besides, non-radiative recombination could be reduced in ultraviolet emission range by controlling the monoethanolamine content.

References

[1] H. Li, J. Wang, H. Liu, C. Yang, H. Xu, X. Li, and H. Cui, "Sol-gel preparation of transparent zinc oxide films with highly preferential crystal orientation," *Vacuum,* 77, 57-62, 2004.

[2] A. Goktas, F. Aslan, A. Tumbul, and S. H. Gunduz, "Tuning of structural, optical and dielectric constants by various transition metal doping in ZnO:TM (TM=Mn, Co, Fe) nanostructured thin films: A comparative study," *Ceram. Int.*, 43, 704-713, 2016.

[3] S. O'Brien, L. H. K. Koh, and G. M. Crean, "ZnO thin films prepared by a singles tep sol–gel process," *Thin Solid Films*, 516, 1391-1395, 2007.

[4] C. Tsay and W. Hsu, "Sol–gel derived undoped and boron-doped ZnO semiconductor thin films: Preparation and Characterization," *Ceram. Int.,* 39, 7425-7432, 2013.

[5] V. Galstyan, E. Comini, C. Baratto, G. Faglia, and G. Sberveglieri, "Nanostructured ZnO chemical gas sensors," *Ceram. Int.*, 41, 14239-14244, 2015.

[6] V. Kumar, R. G. Singh, F. Singh, and L. P. Purohit, "Highly transparent and conducting boron doped zinc oxide films for window of Dye Sensitized Solar Cell applications," *J. Alloy. Comp.,* 544, 120-124, 2012.

[7] M. Wang, W. Liang, Y. Yang, J. Yang, X. Cheng, S. H. Hahn, and E. J. Kim, "Sol-gel derived transparent conducting ZnO:Al thin films: Effect of crystallite orientation on conductivity and self-assembled network texture," *J. Mater Chem. Phys.*, 134, 845-850, 2012.

[8] J. Huang, L. Wang, R. Xu, K.Tang, W. Shi, and Y. Xia, "Growth of p-type ZnO films and fabrication of ZnO photodiode-based UV detectors," *Semicond. Sci. Technol.*, 24, 075025 (5pp), 2009.

[9] E. M. Bachari, G. Baud, S. B. Amor, and M. Jacquet, "Structural and optical properties of sputtered ZnO," *Thin Solid Films*, 348, 165-172, 1999.

[10] D. L. Jiao, X. C. Zhong, W. Q. Qui, H. Zhang, Z. W. Lui, and G. Q. Zhang, "Structure and Electric Conduction in Pulsed Laser-Deposited ZnO Thin Films Individually doped with N, P or Na," *J. Electron. Mater.,* 47, 3521-3528, 2018.

[11] D. Adolph, T. Tinberg, and T. Ive, "Growth of ZnO(0001) on GaN(0001)/4H-SiC buffer layers by plasma-assisted hybrid molecular beam epitaxy," *J. Cryst. Growth,* vol. 426, pp. 129-134, Jun. 2015.

[12] V. K. Ashith, G. K. Rao, S. N. Moger, and R. Smitha, "Effect of post-deposition annealing on the properties of ZnO films obtained by high temperature, micro-controller based SILAR deposition," *Ceram. Int.*, 44, 10669-10676, 2018.

[13] H. L. Ma, Z W. Liu, D. C. Zeng, M. L. Zhong, H. Y. Yu, and E. Mikmekova, "Nanostructured ZnO films with various morphologies prepared by ultrasonic spray pyrolysis and its growing process," *App. Surf. Sci.,* 283, 1006-1011, 2013.

[14] N. T. Son, J. S. Noh, and S. Park, "Role of ZnO thin film in the vertically aligned growth of ZnO nanorods by chemical bath deposition," *App. Surf. Sci.,* 379, 440-445, 2016.

[15] D. Bao, H. Gu, and A. Kuang, "Sol-gel derived c-axis ZnO thin films," *Thin Solid Films*, 312, 37-39, 1997.

[16] Y. Li, L. Xu, X. Li, X. Shen, and A. Wang, "Effect of aging time of ZnO sol on the structural and optical properties of ZnO thin films prepared by sol–gel method," *App. Surf. Sci.,* 256, 4543-4547, 2010.

[17] Y. Babur, A. Tumbul, and M. Yıldırım, "Chemically derived Zn0.90-xMn0.05Fe0.05AlxO thin films: Tuning of crystallite/grain size, optical and dielectric constants and ferromagnetic properties through Al substitutions," *Mater. Sci. Semicond. Process..,* 84, 1-9, 2018.

[18] W. R. Saleh, N. M. Saeed, W. A. Twej, and M. Alwan, "Synthesis Sol-Gel Derived Highly Transparent ZnO Thin Films for Optoelectronic Applications," *Adv. Mater. Phys. and Chem.,* 2, 11-16, 2012.

[19] H. Makino and H. Shimizu, "Influence of crystallographic polarity on the opto-electrical properties of polycrystalline ZnO thin films deposited by magnetron sputtering," *App. Surf. Sci.,* 439, 839-844, 2018.

[20] F. Aslan, A. Tumbul, A. Goktas, R. Budakoglu, and I. H. Mutlu, "Growth of ZnO nanorod arrays by one-step sol–gel process," *J. Sol-Gel Sci. Technol.,* 80, 389-395, 2016.

[21] M. Soylu and M. J. Coskun, "Controlling the properties of ZnO thin films by varying precursor concentration," *J. Alloy. Comp.,* 741, 957-968, 2018.

[22] P. H. Vajargah, V. Abdizadeh, R. Ebrahimifard, and M. R. Golobostanfard, "Sol–gel derived ZnO thin films: Effect of amino-additives," *App. Surf. Sci.,* 285, 732-743, 2013.

[23] A. G. Nunez, S. A. Gil, C. Lopez, P. Roura, and A. Vila, "Role of Ethanolamine on the Stability of a Sol−Gel ZnO Ink," *J. Phys. Chem.*, 121, 23839-23846, 2017.

[24] D. Shikha, V. Metha, S. C. Sood, and J. Sharma, "Structural and optical properties of ZnO thin films deposited by sol–gel method: effect of stabilizer concentration," *J. Mater. Sci.: Mater Electron*, 26, 4902-4907, 2015.

[25] J. Sengupta, R. K. Sahoo, and C. D. Mukherjee, "Effect of annealing on the structural, topographical and optical properties of sol–gel derived ZnO and AZO thin films," *Mater. Lett.,* 83, 84-87, 2012.

[26] V. Kumar, N. Singh, R. M. Mehra, A. Kapoor, L. P. Purohit, and H. C. Swart, "Role of film thickness on the properties of ZnO thin films grown by sol-gel method," *Thin Solid Films*, 539, 161-165, 2013.

[27] L. Spanhel, "Colloidal ZnO nanostructures and functional coatings: A survey," *J. Sol-Gel Sci. Technol.,* 39, 7-24, 2006.

[28] P. Bindu and S. Thomas, "Estimation of lattice strain in ZnO nanoparticles: X-ray peak profile analysis," *J. Theor. Appl. Phys.*, 8, 123-134, 2014.

[29] M. Voigt, M. Klaumünzer, H. Theim, and W. Peukert, "Detailed analysis of the growth kinetics of ZnO Nanorods in methanol," *J. Phys. Chem.*, 114, 49-63, 2010.

[30] R. Zamiri, A. Rebelo, G. Zamiri, A. Adnani, A. Kuashal, M. S. Belsley, and J. M. F. Ferreira, "Far-infrared optical constants of ZnO and ZnO/Ag nanostructures," *RSC Adv.,* 4, 2902-2908, 2014.

[31] J. G. Q. Galvan, I. M. S. Jimenez, H. T. Huitle, L. A. H. Hernandez, F. M. Flores, A. H. Hernandez, E. C. Gonzalez, A. G. Cervantes, A. Z. Angel, and J. J. A. Ibarra, "Effect of precursor solution and annealing temperature on the physical properties of Sol–Gel- deposited ZnO thin films," *Result Phys.,* 88, 1-5, 2013.

[32] X. T. Zhang, Y. C. Liu, Z. Z. Zhi, J. Y. Zhang, Y. M. Lu, D. Z. Shen, W. Xu, G. Z. Zhong, X. W. Fan, and X. G. Kong, "Resonant Raman scattering and photoluminescence from high-quality nanocrystalline ZnO thin films prepared by thermal oxidation of ZnS thin films," *J. Phys. D: Appl. Phys.*, vol. 34, pp. 3430-3433, Dec. 2001.

[33] L. Znaidi, "Sol–gel-deposited ZnO thin films: A review," *Mater. Sci. Eng. B,* vol. 174, pp. 18-30, Jul. 2010.

[34] K. Sivakumar, V. S. Kumar, N. Muthukumarasamy, M. Thambidurai, and T. S. Senthil, "Influence of pH on ZnO nanocrystalline thin films prepared by sol–gel dip coating method," *Bull. Mater. Sci.,* vol. 35, 327-331, 2012.

[35] J. Tauc, *Amorphous and Liquid Semiconductors*, New York: Plenum Press, 1974.